NASA/TM—2018–219866

Repair of Sandwich Structure in Support of the Payload Adapter Fitting

A.T. Nettles, W.E. Guin, and J.R. Jackson
Marshall Space Flight Center, Huntsville, Alabama

S.B. Cox
Kennedy Space Center, Florida

August 2018

The NASA STI Program…in Profile

Since its founding, NASA has been dedicated to the advancement of aeronautics and space science. The NASA Scientific and Technical Information (STI) Program Office plays a key part in helping NASA maintain this important role.

The NASA STI Program Office is operated by Langley Research Center, the lead center for NASA's scientific and technical information. The NASA STI Program Office provides access to the NASA STI Database, the largest collection of aeronautical and space science STI in the world. The Program Office is also NASA's institutional mechanism for disseminating the results of its research and development activities. These results are published by NASA in the NASA STI Report Series, which includes the following report types:

- TECHNICAL PUBLICATION. Reports of completed research or a major significant phase of research that present the results of NASA programs and include extensive data or theoretical analysis. Includes compilations of significant scientific and technical data and information deemed to be of continuing reference value. NASA's counterpart of peer-reviewed formal professional papers but has less stringent limitations on manuscript length and extent of graphic presentations.

- TECHNICAL MEMORANDUM. Scientific and technical findings that are preliminary or of specialized interest, e.g., quick release reports, working papers, and bibliographies that contain minimal annotation. Does not contain extensive analysis.

- CONTRACTOR REPORT. Scientific and technical findings by NASA-sponsored contractors and grantees.

- CONFERENCE PUBLICATION. Collected papers from scientific and technical conferences, symposia, seminars, or other meetings sponsored or cosponsored by NASA.

- SPECIAL PUBLICATION. Scientific, technical, or historical information from NASA programs, projects, and mission, often concerned with subjects having substantial public interest.

- TECHNICAL TRANSLATION. English-language translations of foreign scientific and technical material pertinent to NASA's mission.

Specialized services that complement the STI Program Office's diverse offerings include creating custom thesauri, building customized databases, organizing and publishing research results…even providing videos.

For more information about the NASA STI Program Office, see the following:

- Access the NASA STI program home page at <http://www.sti.nasa.gov>

- E-mail your question via the Internet to <help@sti.nasa.gov>

- Phone the NASA STI Help Desk at 757–864–9658

- Write to:
  NASA STI Information Desk
  Mail Stop 148
  NASA Langley Research Center
  Hampton, VA 23681–2199, USA

NASA/TM—2018–219866

Repair of Sandwich Structure in Support of the Payload Adapter Fitting

A.T. Nettles, W.E. Guin, and J.R. Jackson
Marshall Space Flight Center, Huntsville, Alabama

S.B. Cox
Kennedy Space Center, Florida

National Aeronautics and
Space Administration

Marshall Space Flight Center • Huntsville, Alabama 35812

August 2018

Available from:

NASA STI Information Desk
Mail Stop 148
NASA Langley Research Center
Hampton, VA 23681–2199, USA
757–864–9658

This report is also available in electronic form at
<http://www.sti.nasa.gov>

TABLE OF CONTENTS

LIST OF FIGURES

LIST OF FIGURES (Continued)

LIST OF TABLES

LIST OF ACRONYMS

BVID	barely visible impact damage
CAI	compression after impact
PAF	payload adaptor fitting
SLS	Space Launch System
VID	visible impact damage

NOMENCLATURE

E_c	core compressive modulus, modulus of the carbon/epoxy composite
E_f	facesheet flexural modulus in the direction of loading
K	constant estimated to be 0.82 (best-fit) or 0.33 (lower bound)
P_c	carbon/epoxy composite
P_t	total measured load
t_A	the thickness of the adhesives
t_c	total thickness of composite, core thickness
t_f	thickness
σ_{wrink}	facesheet wrinkling

TECHNICAL MEMORANDUM

REPAIR OF SANDWICH STRUCTURE IN SUPPORT OF THE PAYLOAD ADAPTER FITTING

1. INTRODUCTION

As part of a program examining a composite payload adaptor fitting (PAF) for NASA's Space Launch System (SLS), a repair study of impact damage and misdrilled holes was undertaken. At the beginning of this repair study, the PAF was baselined as a honeycomb sandwich structure with eight-ply quasi-isotropic, carbon-fiber-reinforced epoxy facesheets. Although the baseline configuration could change, the repair program presented herein is generic enough in nature such that it will apply to most sandwich configurations. The vast majority of loads experienced by this structure will be in-plane compression; thus, this repair study concentrates on the in-plane compression strength of representative sandwich structure specimens. The PAF is a truncated cone with a minimum diameter of about 170 in at the top and a maximum diameter of about 335 in at the bottom. While the launch vehicle hardware should be protected throughout its life on the ground, rogue events (or misdrilled holes) are still a possibility. This study is not meant to address large scale damage or damage to the part other than in the acreage (the uniform portion of the structure that does not consist of joints or other detailed areas), but address the most probable type of damages (small impacts and misdrilled holes) in the vast majority of the structure (the acreage).

Results of past studies on repair of composite facesheet sandwich structure are not numerous in the open literature since there are many methods to repair damage, and each end user typically has a preferred methodology that is not necessarily better or worse than what another end user may use for a similar sandwich structure. In general, thin facesheet honeycomb structure (16 plies or less) utilizes patch repairs since scarf repairs are more difficult.[1] Scarf repairs require quite a bit of material to be removed around the damaged area, and if there is no need to remove good material, then attempting to do so can bring about even more problems. For convenience, most repairs are circular, but this is not a requirement, and another shape may be better suited for a given application.

In the open literature, results of the tensile strength of repaired sandwich structure demonstrate that scarf repairs tend to perform better than patch repairs, conversely the opposite was found for compression strength. (Patch repairs tended to give higher strength values than scarf repairs.)[2–6] It should be noted that in these studies, the damage and repair spanned the entire width of the specimens used, representing a 'worst-case' scenario in which the original damaged structure had zero strength.

There are a few papers in the open literature that examined local (not cross-width) repair of compressively loaded sandwich structure.[7–13] Since materials and undamaged strength measurements greatly vary, a direct comparison is not possible, but in general, the repairs (either patch or scarf) did improve the compression strength of the sandwich structure over those that had been damaged and not repaired.

One of the difficulties of assessing how much undamaged compression strength is recovered due to a repair is in measuring what the 'true' undamaged compression strength of the sandwich structure is. Multiple failure modes, as well as sensitivity to specimen machining and uniform application of load, make this difficult. For example, obtaining artificially low values for undamaged compression strength will give the appearance that repairs are more efficient than they truly are. The problem of obtaining a true undamaged compression strength of sandwich structure will be addressed later in this Technical Memorandum.

2. SPECIMENS USED IN THIS STUDY

The acreage of the PAF was baselined as 8-ply quasi-isotropic IM7/8552-1 carbon/epoxy facesheets on each side of 1-in-thick 4.5 lb/ft^3 density aluminum honeycomb. An epoxy film adhesive (FM209-1M) was used between the core and facesheets, which were fiber placed and subsequently autoclave cured at 40 psi. The baseline sandwich structure configuration used in this study is intended to be general in nature. As such, although the configuration considered herein may ultimately change to accommodate different variants of the PAF, this study is thought to be generic enough such that it can be applied to a range of PAF configurations.

Since it has been demonstrated that panel curvature and size has little effect on compression after impact (CAI) strength of sandwich structure,[14] it was decided that flat panels of minimal size could be used. A typical cross-section of the sandwich structure used in this study is shown in figure 1.

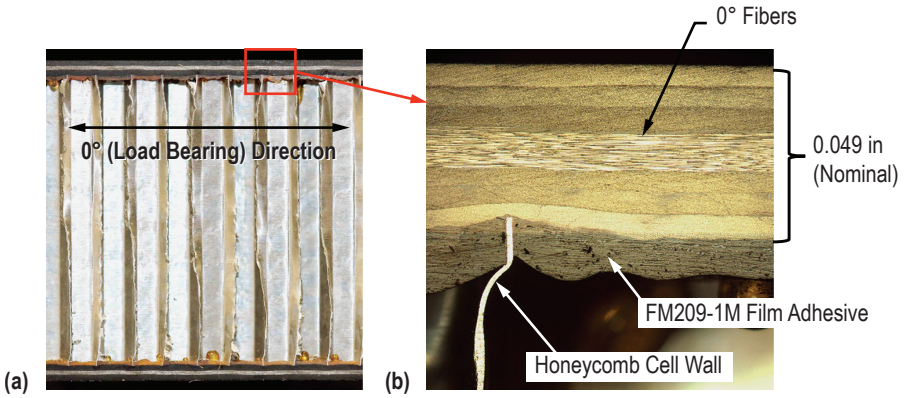

Figure 1. Polished cross-section of honeycomb sandwich structure used in this study: (a) complete thickness of sandwich structure and (b) closeup of facesheet.

There appears to be a small amount of waviness of the load-bearing 0º fibers, which is typical of co-cured honeycomb sandwich structure. The nominal thickness of the facesheets was 0.049 in based on numerous optical microscopic measurements. As can be seen in figure 1b, the facesheet is at its thinnest at the cell wall and at its thickest between cell walls. An average of 50 random thickness measurements were averaged to arrive at the 0.049-in thickness value.

2.1 Determining Undamaged Compression Strength

Before assessing how much compression strength can be recovered due to a repair, the compression strength of undamaged sandwich structure needs to be ascertained. This is not a simple task as multiple failure modes are possible for end-loaded sandwich structure. 'Valid' failure modes include (1) face dimpling, (2) panel buckling, (3) shear crimping, (4) face wrinkling, and (5) face-material failure. A thorough explanation of these along with methods to calculate each are given in reference.[15] Of these five failure modes two (face wrinkling and face-material failure) were predicted to occur at a much lower value than the other three.

2.1.1 Face Wrinkling

Using the methodology in reference 15 the approximate stress (best first estimate) at which face wrinkling may occur is given by:

$$\sigma_{wrink} = K(E_f)\left(\frac{t_f E_c}{E_f t_c}\right)^{0.5} , \tag{1}$$

where

t_f = thickness
t_c = core thickness
E_f = facesheet flexural modulus in the direction of loading
E_c = core compressive modulus.

K is a constant that has been estimated by experiments to be 0.82 (best-fit) or 0.33 (lower bound). This will give a large range of values and is thus not very accurate. Note that the flexural, rather than in-plane modulus of the facesheet, is used since this value is usually not the same for laminated composites as it is for homogeneous materials.

The value of facesheet thickness was measured using digital microscopy and found to have a nominal value of 0.049 in, and the flexural modulus of the facesheet was calculated as 3.3 Msi. For comparison, the in-plane modulus was calculated (and measured) as 8.3 Msi. The core thickness was 1 in, and the compressive modulus of the core was taken from vendor data as 150 ksi. This gives an approximate face wrinkling stress of 128 ksi (best fit) or 51 ksi (lower bound).

2.1.2 Face Material Compression Failure

The ideal upper limit of compression strength of the facesheets can be estimated using published data. The highest, and thus most correct (since specimens are difficult to make 'artificially strong'), are typically supplied by the vendor, as referenced in "An Account of One Engineer's Long-Term Involvement with Aerospace Applications of Composite Structures," Boeing Paper PWDM05-0089, (not publicly available) by L.J. Hart-Smith. The compressive strain-to-failure of

unidirectional IM7/8552 is given as 1.3% and using classical lamination theory the modulus of a quasi-isotropic lay-up is 8.3 Msi. Thus, the stress at 1.3% compression strain is 107 ksi, assuming linear elastic behavior. Achieving this compression strength is unlikely since the facesheets are co-cured, and thus some waviness of the load-bearing 0º fibers can be expected, which can reduce the compression strength of a laminate from one that has no waviness. The best way to measure the compression strength of the as-manufactured facesheets is to eliminate the honeycomb from the test method to preclude any other failure modes (such as facesheet wrinkling described in the previous section) and maintain simplicity in specimen preparation and test technique. The technique used in this study to achieve this was to cut the facesheets off of the aluminum honeycomb with a band saw and then machine off any residual core material down to the adhesive layer that was used to join the facesheet to the honeycomb. Machining off the adhesive down to the first carbon/epoxy ply was not feasible since the surface was not flat but dimpled due to co-curing over the honeycomb, and machining this surface flat would have damaged carbon fibers. The resulting pair of facesheets are now asymmetrical due to this adhesive layer, which causes the facesheets to incur a curvature. A photograph of the facesheets of a specimen with the core removed is shown in figure 2.

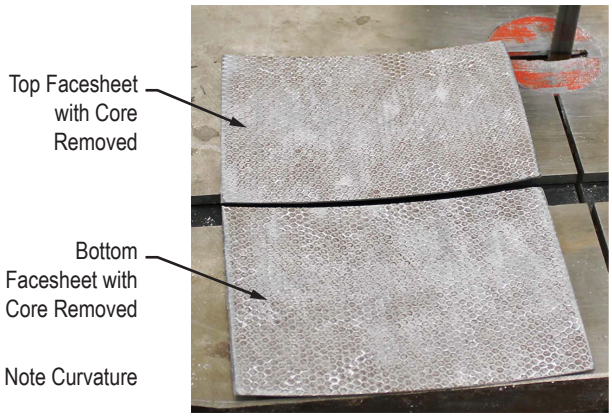

Figure 2. Photograph of facesheets after removal of core.

To regain symmetry, the two halves were bonded together (concave sides together) with EA 9394 epoxy paste adhesive and placed in a platen press during cure. After the paste adhesive had cured, the resulting flat panel was machined into specimens to be tested by the combined loading compression method according to ASTM D6641. A specimen and a closeup view of its edge are shown in figure 3. As can be seen, some residual pieces of core are still embedded in the adhesive layer.

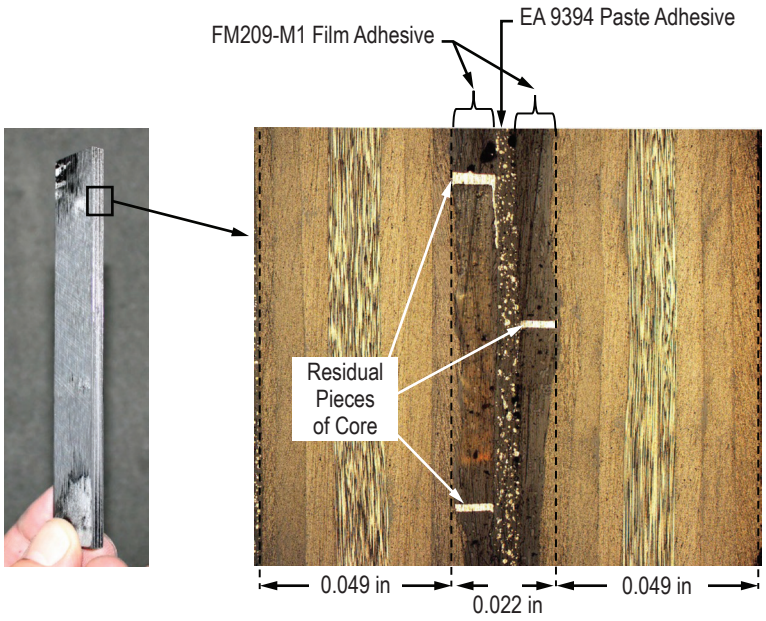

Figure 3. Photograph of CLC test specimen made from two facesheets with core removed and closeup of edge.

The adhesives joining the two halves of carbon/epoxy laminate carries a small amount of load during compression loading. Using the rule of mixtures shows that the load carried by the carbon/epoxy composite P_c as a function of total measured load P_t is given by:

$$P_c = P_t\left(\frac{t_c E_c}{t_c E_c + t_A E_A}\right) , \tag{2}$$

where

E_c = modulus of the carbon/epoxy composite,
E_A = the modulus of the epoxy adhesives (which are approximately equal)
t_c = total thickness of the composite (2×0.049 in)
t_A = the thickness of the adhesives.

Using E_c = 8.3, Msi, E_A = 0.6 Msi, t_c = 0.098 in, and t_A = 0.022 in, the facesheet compression strength results for seven specimens tested are presented in table 1.

Table 1. Results of compression strength testing of the facesheets.

Specimen No.	Width (in)	P_t (lb)	P_c (lb)	$Ac = t_c \times$Width (in^2)	σ_c (ksi)
1	0.580	5,587	5,475	0.0568	96.3
2	0.578	5,548	5,437	0.0566	96.1
3	0.574	5,653	5,540	0.0563	98.4
4	0.475	4,854	4,757	0.0466	102.1
5	0.487	4,677	4,583	0.0477	96.1
6	0.482	4,884	4,786	0.0472	101.4
7	0.490	4,739	4,644	0.0480	96.8
				Average	98.2 ± 2.6

The average value of 98.2 ksi represents an upper limit of what can be measured as the facesheet strength of undamaged honeycomb specimens. As will be seen, this value was not achieved, perhaps due to face wrinkling failures (predicted to possibly occur as low as 51 ksi).

2.1.3 Sandwich Structure Compression Strength

For undamaged, damaged, and repaired sandwich structure testing, the same type specimen was used. A schematic of the specimen is shown in figure 4. In order to prevent end brooming of the specimens (an invalid failure mode), the ends were potted using wood inserts with an epoxy paste adhesive, and tabs of carbon/epoxy were bonded to the ends to help distribute the load at the ends of the facesheets.

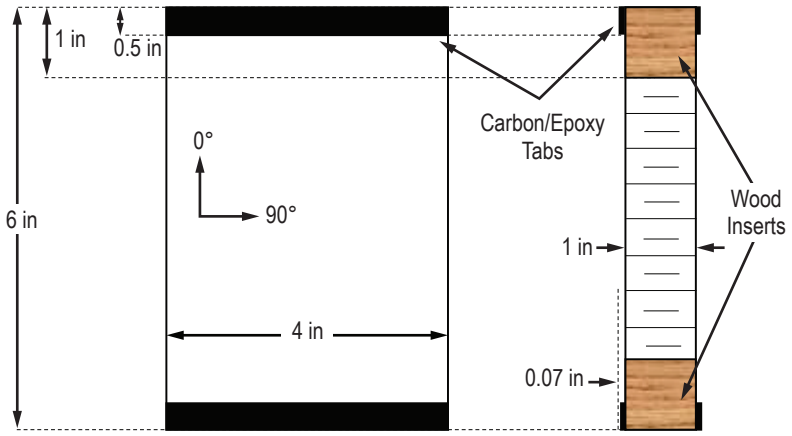

Figure 4. Schematic of specimen used in this study.

Strain gages were placed on both sides of the specimen to ensure even loading of each of the facesheets. The specimens were taken to approximately 2,000 microstrain, and if one side was lower than the other, shims were placed under the edge that was reading low until the gages were

even. During compression testing, the gages were monitored, and if any deviation greater than 10% occurred, the test was stopped, and shims would be rearranged until the gages read within 10% of each other all the way until failure of the specimen.

Results of compression testing of undamaged specimens of sandwich structure are given in table 2. It was not possible (even with high-speed video) to ascertain if the failures were due to face wrinkling, facesheet-material failure, or some other mechanism. Of practical interest is the maximum load these specimens can carry and how much of this load could be recovered by the repair methods reported in this study.

Table 2. Results of compression testing of sandwich structure used in this study.

Specimen No.	Width (in)	Load at Failure (lb)	Stress at Failure (ksi)
Undamaged-1	3.70	28,058	77.4
Undamaged-2	3.98	29,328	75.3
Undamaged-3	3.92	28,985	75.5
Undamaged-4	3.72	30,166	82.7
Undamaged-5	3.65	26,658	74.5
Undamaged-6	3.65	28,240	78.9
Undamaged-7	3.35	26,946	82.1
		Average	78.1 ± 3.3

A photograph of a typical failed undamaged specimen is given in figure 5. The zone of breakage at or near where the wood inserts ended within the specimens was consistent for each test. Numerous techniques were attempted in an effort to eliminate any stress concentrations being induced at this zone, but none gave higher compression strengths. As can be seen, getting the full 98.2 ksi strength out of the facesheets was not achieved. Given that the face-wrinkling stress could be as low as 51 ksi (as calculated earlier) and past experience with compression testing sandwich structure, this is not a surprising result. The average compression strength result of 78.1 ksi obtained for these specimens is higher than the average compression strength of similar sandwich structures tested elsewhere.[13]

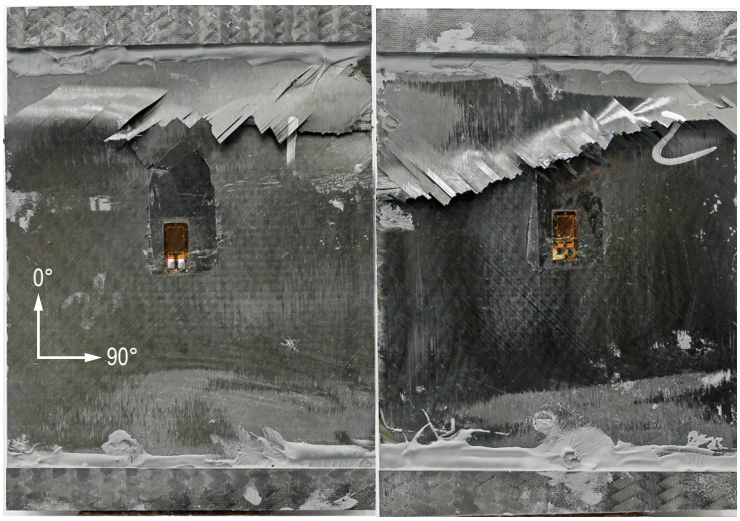

Figure 5. Photograph of both sides of compression failure of undamaged specimen.

2.2 Damaged Specimens

2.2.1 Holes

Specimens like those used for undamaged testing were tested with a 0.25-in-diameter hole drilled through one of the facesheets. The results are given in table 3. A photograph of compression failure caused by a hole is shown in figure 6. All failures were located at the hole as expected.

Table 3. Results of open-hole compression testing of sandwich structure used in this study.

Specimen No.	Width (in)	Load at Failure (lb)	Stress at Failure (ksi)
Hole-1	4.043	15,868	40.1
Hole-2	4.355	17,822	41.6
Hole-3	4.470	17,650	40.1
Hole-4	4.561	19,289	43.0
Hole-5	4.411	19,213	44.3
Hole-6	4.400	20,808	48.1
Hole-7	4.452	19,481	44.5
Hole-8	4.315	17,956	42.5
		Average	43.0 ± 2.6

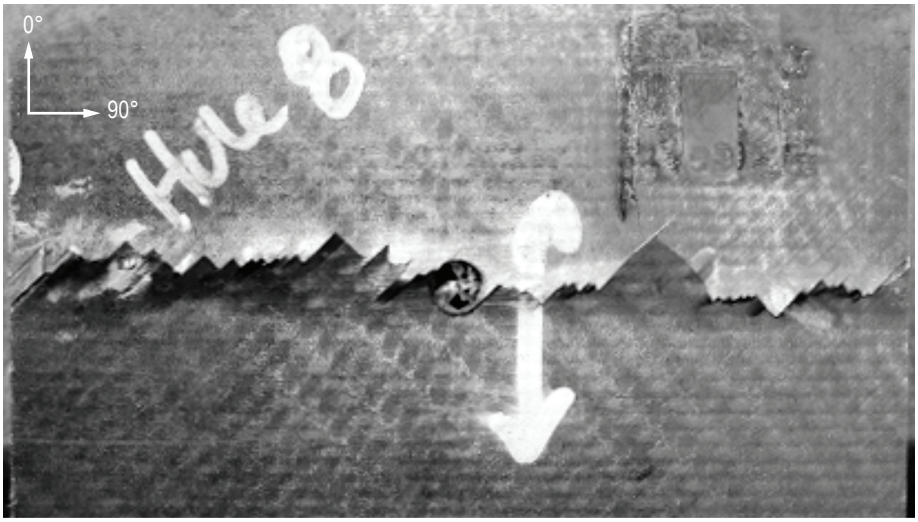

Figure 6. Photograph of failure zone of an open-hole compression specimen.

2.2.2 Barely Visible Impact Damage

Specimens were impacted with about 2.4 ft•lb of energy with a 0.5-in-diameter impactor. This impact severity level has been determined to be the 'barely visible impact damage' (BVID) threshold. A photograph of a specimen impacted with 2.4 ft•lb with a 0.5-in impactor, along with its thermography signature, is shown in figure 7. Table 4 gives the CAI strength results of the seven specimens impacted with BVID.

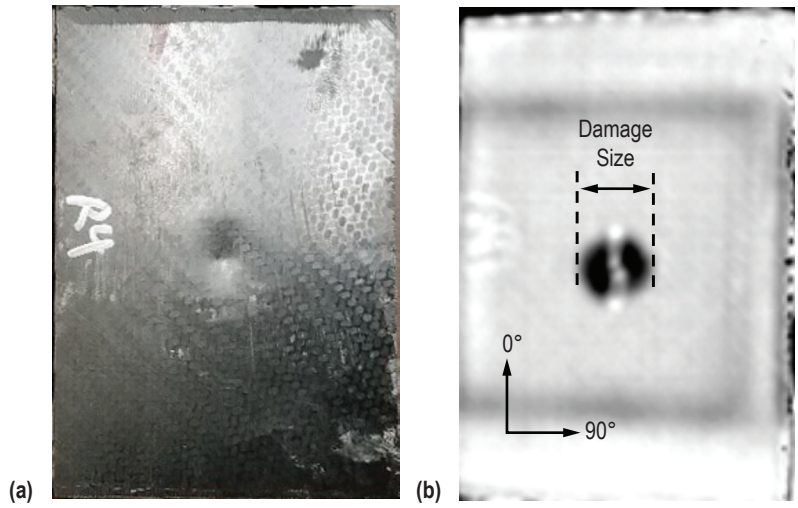

Figure 7. Images of sandwich specimen impacts with 2.4 ft•lb (BVID): (a) photograph and (b) thermograph.

Table 4. Measured compression strength of BVID impact specimens.

Specimen No.	Impact Energy (ft•lb)	Max Load of Impact (lb)	Dent Depth (in)	Damage Size (in)	Compression Strength (ksi)
BVID-1	No data	No data	0.0115	1.01	52.0
BVID-2	2.36	524	0.0110	1.01	51.7
BVID-3	2.40	537	0.0140	1.01	51.4
BVID-4	2.41	505	0.0100	1.00	49.0
BVID-5	2.24	498	0.0120	0.97	53.9
BVID-7	2.22	500	0.0140	1.01	53.6
BVID-8	2.22	482	0.0115	1.00	58.9
				Average	52.9 ± 3.1

The size of damage (width direction) for BVID as indicated by the thermography results was about 1 in. A photograph of compression failure caused by BVID is shown in figure 8. As expected, all failure zones were located through the area of impact damage.

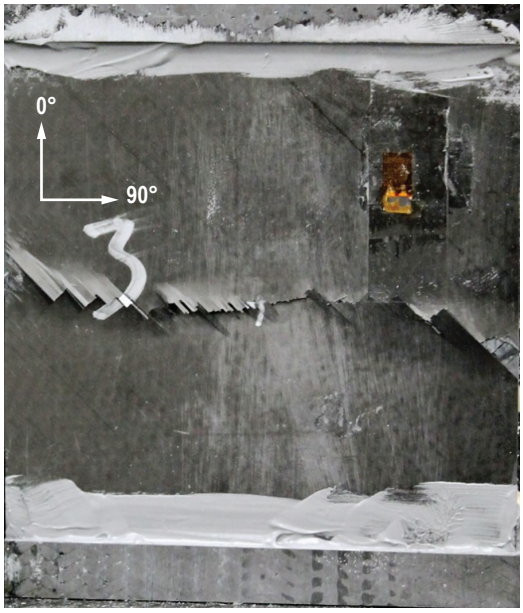

Figure 8. Photograph of a failed BVID compression specimen.

2.2.3 Visible Impact Damage

Easily visible impact damage (VID) has been defined as 7.4 ft•lb with a 0.5-in impactor. Table 5 shows the results of CAI testing of three specimens with VID. The average size of damage was about 1.3 in. A photograph of a specimen impacted with 7.4 ft•lb with a 0.5-in impactor, along with its thermography signature, is shown in figure 9. A photograph of compression failure caused by VID is shown in figure 10. As expected, all failures were through the impact damage zone.

Table 5. Measured compression strength of VID impact specimens.

Specimen	Impact Energy (ft • lb)	Max Load of Impact (lb)	Dent Depth (in)	NDE Width (in)	Compression Strength (ksi)
VID-1	7.40	656	0.0340	1.25	49.2
VID -2	7.42	756	0.0375	1.37	44.8
VID -3	7.41	732	0.0385	1.23	43.5
				Average	45.8 ± 3.0

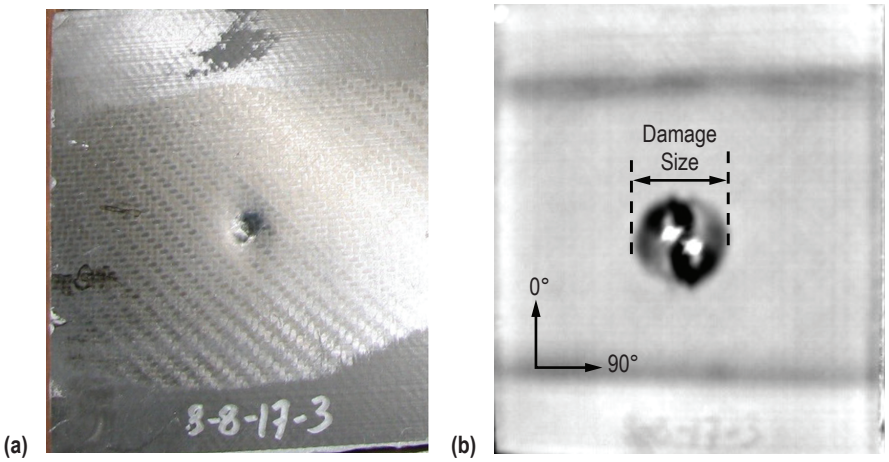

Figure 9. Images of sandwich specimen impacted with 7.4 ft•lb (VID): (a) photograph and (b) thermograph.

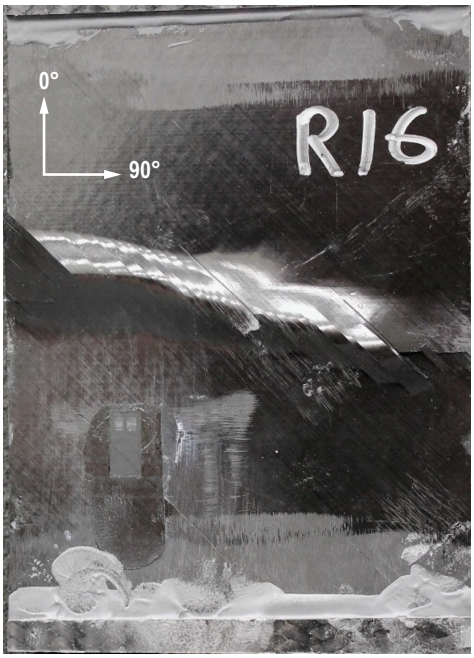

Figure 10. Photograph of a failed VID compression specimen.

3. REPAIR

3.1 Misdrilled Holes

Since damage may need to be repaired, it was introduced into sandwich specimens, and repairs were made to assess how much of the original strength could be regained. The first repairs were done on specimens with holes since misdrilled holes in the hardware are possible. Simple patch repairs consisting of eight plies of T650/5320-1 out-of-autoclave carbon/epoxy unidirectional prepreg were used for the repairs. The holes were first filled with epoxy resin to prevent the patch from draping into the hole during cure. Once the holes were filled with epoxy and the epoxy had cured, the surface of the specimens to which the repair was to be bonded was prepared by abrading until the outermost fibers in the top layer were visible. The patches had the same layup as the parent laminate ([45/90/–45/0]S). FM 300-2M film adhesive was used between the patches and the specimens to aid in adhesion. The plies of the patches were made successively smaller by 0.25 in per ply to minimize edge effects. The patches were circular with an outermost diameter of 3.5 in (innermost diameter of 2 in). Thus, the smallest ply of the patch was about twice as large as the damage zone for BVID specimens and 1.5× as big as the damage zone for VID specimens. The patches were applied with the smaller plies close to the specimen ('reverse wedding cake') as shown schematically in figure 11. The resulting specimens were vacuum bagged and cured per the manufacturer's recommendation in an air-circulating programmable oven. Vacuum was held at a nominal value of 13.9 psi. A photograph of a repaired specimen in shown in figure 12. The results of compression testing of specimens with repaired holes are given in table 6.

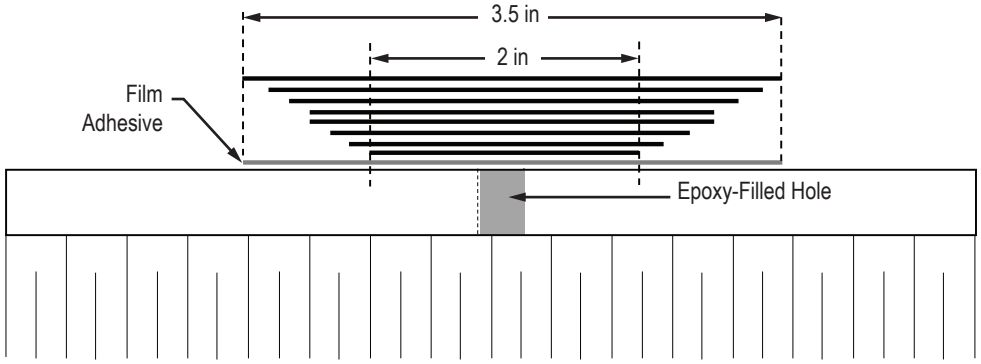

Figure 11. Schematic of 'reverse wedding cake' repair.

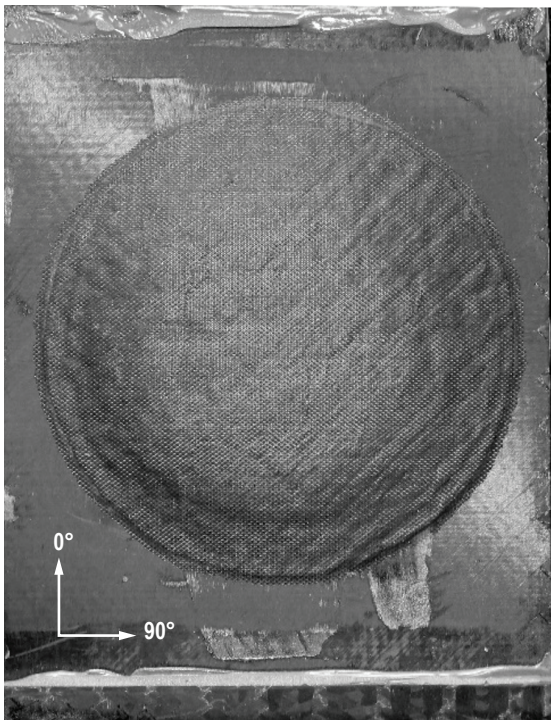

Figure 12. Photograph of repaired specimen.

Table 6. Results of compression testing of specimens with holes (repaired).

Specimen No.	Width (in)	Load (lb)	Ultimate Stress (ksi)	Failure at Hole?
Hole Repair 1	4.15	33,368	82.1	Yes, patch remained intact
Hole Repair 2	4.13	32,780	80.9	No
Hole Repair 3	3.84	30,042	79.9	No
Hole Repair 4	3.97	27,709	71.1	No
Hole Repair 5	4.00	35,374	90.4	No
Hole Repair 6	3.89	27,806	73.0	No
		Average	79.6 ± 6.9	

A photograph of a failed specimen that did not fail at the hole is shown in figure 13. These failures were very much like those of the undamaged specimens as noted in figure 5. The resulting compression strength values were essentially the same as undamaged specimens.

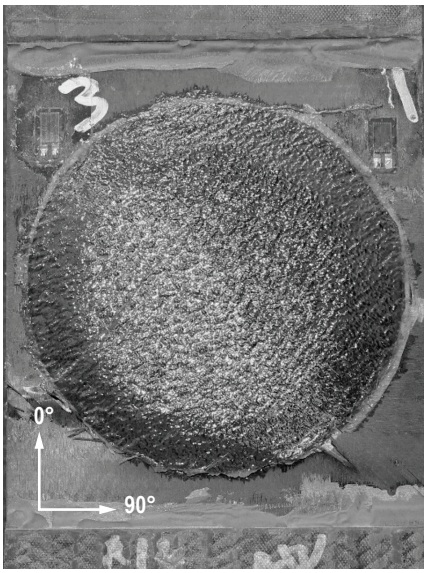

Figure 13. Photograph of specimen that did not fail at hole.

3.2 Barely Visible Impact Damage

The same repair method used to repair holes (previous section) was used to repair specimens with BVID. At first, the film adhesive and patches were applied to the impact-damaged laminate without removing or filling the damage zone. To keep the repair process as simple as possible, the damaged material was not removed in the hopes that the patch would redistribute the load around the damage zone, just as it did for holes as found in the previous section. The core does not carry any appreciable shear loads, thus the core damage should not interfere with the end-loaded compression strength. Since the core damage is localized, the gross section compression modulus of the core E_c is not effected, and equation (1) should not be altered by the core damage. (If the sandwich structure needed to carry shear loads, then the core would have to be repaired.) It has been shown that impact damage and holes fail due to similar failure mechanisms in end-loaded sandwich structure,[16] so this approached seemed feasible. Two specimens were tested in this manner, and the results gave compression strengths of 66.8 and 58.2 ksi. This represents an improvement over the impact damaged nonrepaired average strength of 52.9 ksi, but not up to the strength obtained from the repaired holes. The failure location for both of these specimens was on the unimpacted side of the specimens, indicating that the repair was not carrying the amount of load it should (i.e., it was 'soft,' and dumped excess load onto the undamaged facesheet but was carrying enough load to preclude failure through the damage zone.) Since the impact damage causes a dent in the specimen. It was suspected that the patch conformed to this dent during cure, so the 0° load bearing fibers were not as straight as desired and thus had reduced stiffness but sufficient strength to keep the damage zone from causing failure.

To stiffen the patch in order to reduce the amount of load being carried by the undamaged facesheet, the next set of specimens had the dent filled smooth with epoxy resin before applying the film adhesive and patch. A photograph of an impacted specimen with the dent filled flush to the surface with epoxy is shown in figure 14. A cross section of this type of repair is shown in figure 15. The distinct zones of damaged parent material, epoxy filler, and patch are labeled. Table 7 lists the results of the compression strength of these repaired specimens.

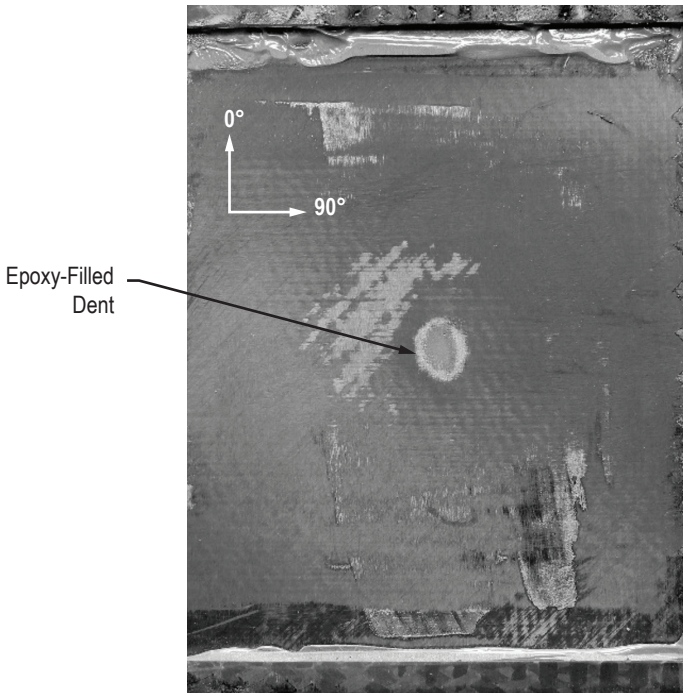

Figure 14. Photograph of BVID dent filled and smoothed with epoxy.

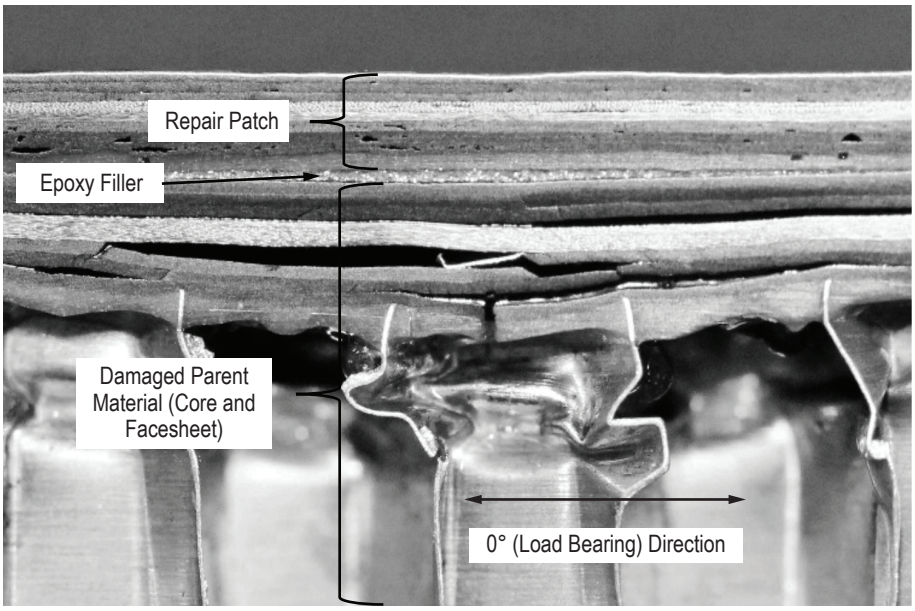

Figure 15. Cross-section of BVID repair.

Table 7. CAI results of patch-repaired BVID specimens.

Specimen No.	Impact Energy (ft•lb)	Maximum Load of Impact (lb)	Dent Depth (in)	NDE Width (in)	CAI Strength (ksi)	Region of Failure
BVID Repair-4	2.46	585	0.0155	0.71	82.1	Bottom between tab and repair
BVID Repair-5	2.48	612	0.0150	1.01	87.2	Bottom between tab and repair
BVID Repair-6	2.45	628	0.0110	0.97	81.5	Broke at repair
BVID Repair-8	2.45	624	0.0140	1.01	85.4	Broke at repair
BVID Repair-9	2.43	583	0.0150	1.00	90.5	Bottom between tab and repair
				Average	85.3 ± 3.7	

A photograph of a failed specimen that failed between the tab and repair is shown in figure 16. These failures were very much like those of the undamaged specimens as noted in figure 5. The average resulting compression strength values were a little higher than those of the undamaged specimens but not enough to cause a statistically significant difference (within standard deviations).

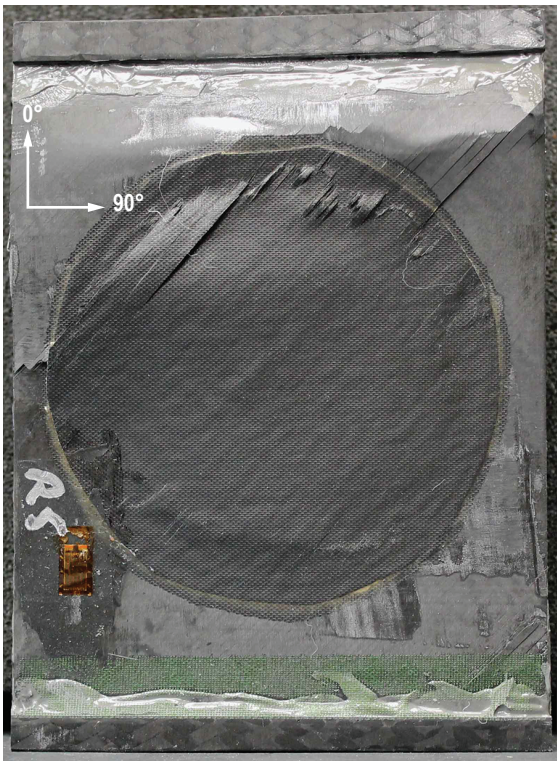

Figure 16. Typical failure of patch-repaired BVID specimens.

3.3 Visible Impact Damage

Since the results of the simple patch repairs on BVID were so encouraging, it was next determined if the same methodology could be used to repair sandwich structure that had sustained more severe damage.

The initial repair methodology of these highly damaged sandwich specimens was similar to that used for BVID. The dent due to impact was filled with epoxy, and then the surface ground flat down to the outermost fibers. The type of patch used for the BVID and hole repairs was the same for these specimens that contained VID. A cross-section of a repair of a VID specimen is shown in figure 17. The distinct zones of damaged parent material, epoxy filler, and patch are labeled. Table 8 lists the results of the compression strength of these repaired specimens.

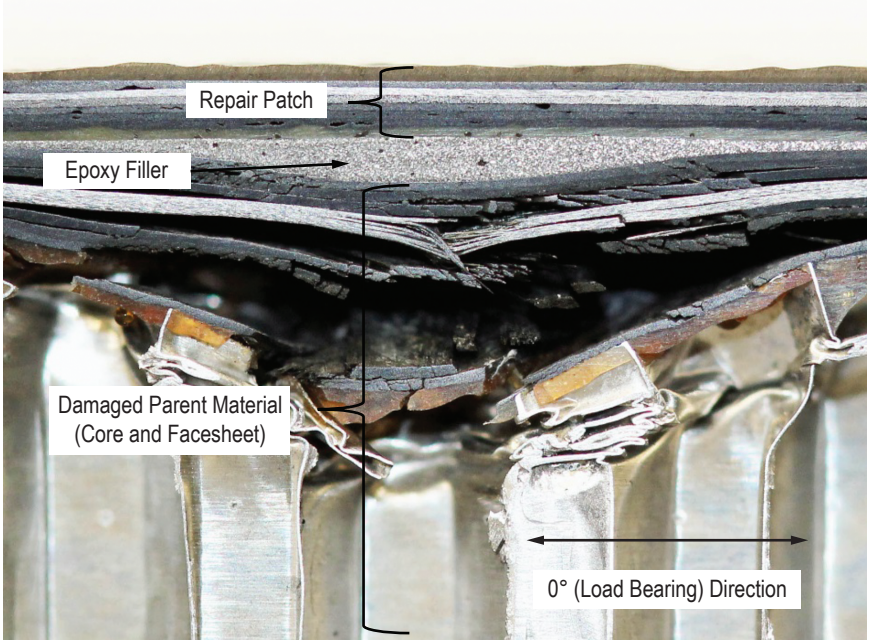

Figure 17. Cross-section of repaired damage caused by 7.5 ft•lb impact.

Table 8. CAI results of patch-repaired VID specimens.

Specimen No.	Impact Energy (ft•lb)	Maximum Load of Impact (lb)	Dent Depth (in)	NDE Width (in)	CAI Strength (ksi)	Region of Failure
VID Repair-1	7.55	760	0.067	1.23	71.5	At damage site through patch
VID Repair-2	7.53	734	0.068	1.18	68.3	At damage site through patch
VID Repair-3	7.55	762	0.063	1.24	74.7	Broke at top
VID Repair-4	7.53	776	0.059	1.20	74.7	Broke at bottom
VID Repair-5	7.51	769	0.055	NP*	64.3	Under patch
VID Repair-6	7.47	774	0.056	NP	70.6	At damage site through patch
VID Repair-7	7.60	769	NP	NP	73.4	Broke at bottom
VID Repair-8	7.54	755	NP	NP	72.6	Broke at bottom
				Average	71.3 ± 3.5	

*NP = Not performed.

A photograph of a failed specimen that failed under the patch is shown in figure 18, and one that failed through the patch is shown in figure 19. The resulting compression strength values were lower than undamaged specimens (outside the limits of standard deviations).

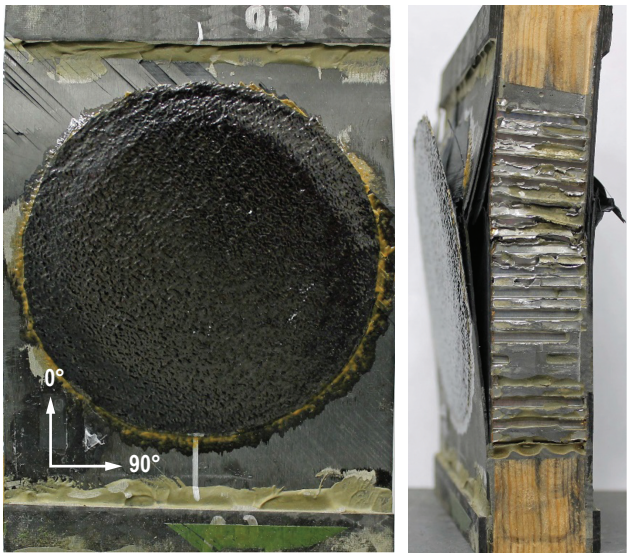

Figure 18. Failure of repaired VID specimen that failed under the patch (front and side views).

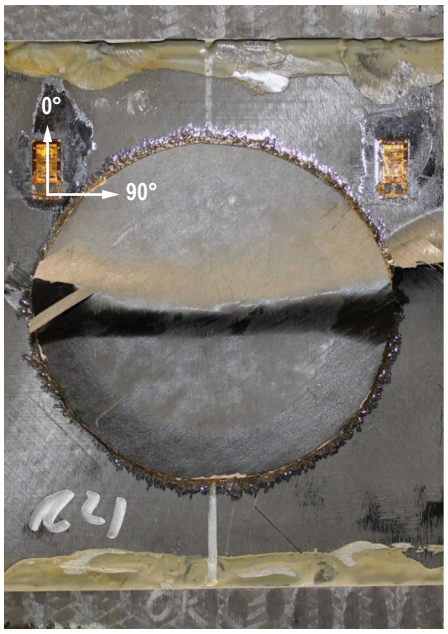

Figure 19. Example of through-patch failure for repaired VID specimen.

4. SUMMARY AND CONCLUSIONS

A summary visual representation of the compression strength data generated in this study is presented in figure 20. Variability is indicated by the standard deviation lines at the top of each bar.

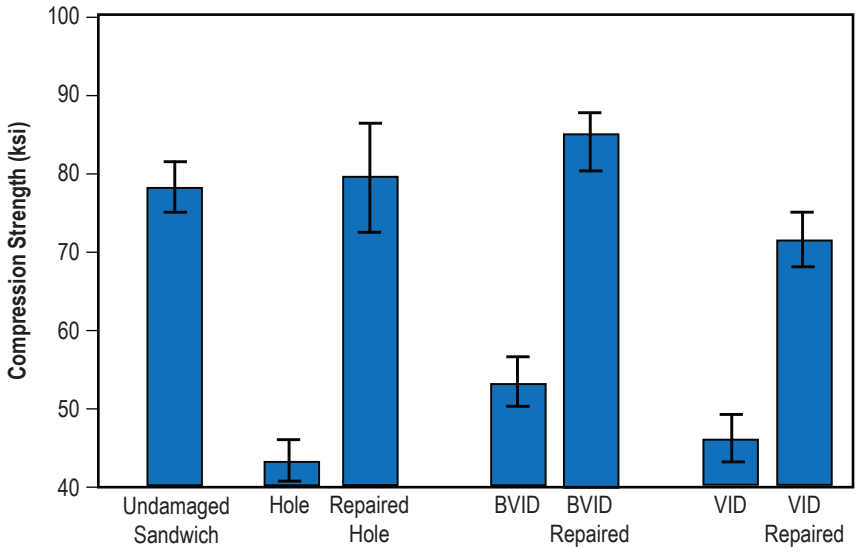

Figure 20. Bar chart summary of compression strength results from this study.

For the sandwich structures tested in this study, the conclusion is simple patch repairs without removal of the damaged material can be used to regain all of the original strength of the panel for 0.25-in holes and BVID. For VID, about 91% of the original strength was regained. Since failures on most of these tests were through the damage zone, it suggests that the patches were not quite sufficient enough to regain 100% of the undamaged load-carrying capability. Bigger patches are probably needed, such that the size of the smallest layer in the patch is twice as big as the damage (as it was for the BVID specimens). This indicates that the smallest layer in a patch to repair VID needs to have a diameter of at least 2.6 in rather than 2 in as used in this study.

This study shows that for 0.25-in holes and BVID tested in this study, it is not necessary to remove the damaged material, suggesting that the repair patch will carry load such that the damage zone will not propagate and cause specimen failure. Not having to remove the damaged area is likely also true for VID, but until it is shown that all undamaged compression strength is returned by utilizing larger patches, this cannot be unequivocally stated. Surface irregularities (holes and dents) are also shown to need to be filled such that a co-cured repair patch will not conform to these irregularities and soften the patch due to waviness of the load bearing fibers in the patch.

Establishing a pristine compression strength of the sandwich structure to compare to the repairs is difficult. This difficulty is evident by the sandwich structure's inability to achieve the compression strength of the facings without the core being involved in the test methodology.

REFERENCES

1. Baker, A.A. and Scott, M.L.: "Repair Technology," in *AIAA Education Series, Composite Materials for Aircraft Structures, Third Edition*, doi:10.2514/4.103261, 400 pp., American Institute of Aeronautics and Astronautics, August 2016.

2. Stone, R.H.: "Repair techniques for graphite/epoxy structures for commercial transport applications," NASA CR-159056, NASA Langley Research Center, Hampton, VA, 212 pp., January 1983.

3. Ahn, S.-H. and Springer, G.S.: "Repair of Composite Laminates-I: Test Results," *J. Compos. Mater.*, Vol. 32, No. 11, pp. 1036–1074, June 1998.

4. Ghazali, E.; Dano, M.L.; Gakwaya, A.; and Amyot, C.O.: "Mechanical performance of repaired sandwich panels: Experimental characterization and finite-element modelling," *J. Sandw. Struct. Mater.*, doi:10.1177/1099636217716059, July 2017.

5. Mahdi, S.; Kinloch, A.J.; Matthews, F.L.; and Crisfield, M.A.: "The Static Mechanical Performance of Repaired Composite Sandwich Beams: Part I-Experimental Characterisation," *J. Sandw. Struct. Mater.*, Vol. 5, No. 2, pp. 179–202, April 2003.

6. Kirollos, B.W.M.; Trede, R.; and Lampen, P.: "The experimental static mechanical performance of ironed repaired GFRP-honeycomb sandwich beams," *J. Sandw. Struct. Mater.*, Vol. 14, No. 6, pp. 694–714, September 2012.

7. Charalambides, M.N.; Hardouin, R.; Kinloach, A.J.; and Matthews, F.L.: "Adhesively-bonded repairs to fibre-composite materials I: Experimental," *Composites Part A*, Vol. 29, No. 11, pp. 1371–1381, November 1998.

8. Ushakov, A.; Stewart, A.; Mishulin, I.; and Pankov, A.: "Probabalistic Design of Damage Tolerant Composite Aircraft Structures," DOT/FAA/AR-01/55, U.S. Department of Transportation, Federal Aviation Administration, Springfield, VA, 200 pp., January 2002.

9. Bull, P.H. and Hallstrom, A.: "High-velocity and Quasi-Static Impact of Large Sandwich Panels," *J. Sandw. Struct. Mater.*, Vol. 6, No.2, pp. 97–113, March 2004.

10. Park, H.: "Investigation on Repairable Damage Tolerance for Structural Design of Aircraft Composite Structure," *J. Compos. Mater.*, doi:10.1177/0021998316643579, April 2016.

11. Liu, S.; Guan, Z.; Guo, X.; Sun, K.; and Kong, J.: "Edgewise compressive performance of repaired composite sandwich panels – Experiment and finite element analysis," *J. Reinf. Plast. Compos.*, Vol. 32, No. 18, pp. 1331–1347, doi:10.1177/2F0731684413487780, September 2013.

12. Raju, M.; Reddy, C.; Swamy, M.; Giridhar, G.; Srikanth, L.; Prakash, M.; and Rao, R.: "Repair Effectiveness Studies on Impact Damaged Sandwich Composite Constructions," *J. Reinf. Plast. Compos.*, Vol. 25, No. 1, pp. 5–10, January 2006.

13. Cox, S.: "Composite Structures Repair Development at Kennedy Space Center," Paper Presented at the *LSU College of Engineering Sidney E. Fuchs Seminar Series*, Baton Rouge, LA, 36 pp., November 2015.

14. Moody, R.C. and Vizzini, A.J.: "Test and Analysis of Composite Sandwich Panels With Impact Damage," DOT/FAA/AR-01/124, U.S. Department of Transportation, Federal Aviation Administration, Springfield, VA, 67 pp., May 2002.

15. Sullins, R.T.; Smith, G.W.; and Spier, E.E.: "Manual for structural stability analysis of sandwich plates and shells," NASA-CR-1457, NASA, Washington, D.C., 387 pp., December 1969.

16. Nettles, A.T. and Scharber, L.L.: "The Influence of GI and GII on the Compression After Impact Strength of carbon Fiber/Epoxy Laminates and Sandwich Structure," NASA TP/2017-219635, NASA Marshall Space Flight Center, Huntsville, AL, 40 pp., July 2017.

REPORT DOCUMENTATION PAGE

Form Approved
OMB No. 0704-0188

1. REPORT DATE *(DD-MM-YYYY)*	2. REPORT TYPE	3. DATES COVERED *(From - To)*
01–08–2018	Technical Memorandum	

4. TITLE AND SUBTITLE

Repair of Sandwich Structure in Support of the Payload Adapter Fitting

5a. CONTRACT NUMBER

5b. GRANT NUMBER

5c. PROGRAM ELEMENT NUMBER

6. AUTHOR(S)

A.T. Nettles, W.E. Guin, J.R. Jackson, and S.B. Cox*

5d. PROJECT NUMBER

5e. TASK NUMBER

5f. WORK UNIT NUMBER

7. PERFORMING ORGANIZATION NAME(S) AND ADDRESS(ES)

George C. Marshall Space Flight Center
Huntsville, AL 35812

8. PERFORMING ORGANIZATION REPORT NUMBER

M–1470

9. SPONSORING/MONITORING AGENCY NAME(S) AND ADDRESS(ES)

National Aeronautics and Space Administration
Washington, DC 20546–0001

10. SPONSORING/MONITOR'S ACRONYM(S)

NASA

11. SPONSORING/MONITORING REPORT NUMBER

NASA/TM—2018–219866

12. DISTRIBUTION/AVAILABILITY STATEMENT

Unclassified-Unlimited
Subject Category 24
Availability: NASA STI Information Desk (757–864–9658)

13. SUPPLEMENTARY NOTES

Prepared by the Damage Tolerance Assessment Branch, Engineering Directorate
*Kennedy Space Center, FL

14. ABSTRACT

Experiments were done using sandwich structure typical of launch vehicle Payload Adapter Fitting. Specimens with 8-ply quasi-isotropic carbon/epoxy facesheets and aluminum honeycomb core were damaged with representations of misdrilled 0.25-in diameter holes, barely visible impact damage (BVID) and visible impact damage (VID). A simple patch repair technique not requiring removal of any material is presented and assessed for residual compressive load-carrying capability. Edgewise compression tests on repaired specimens demonstrated repairs could recover all compressive load-carrying capability of the misdrilled hole, BVID specimens, and about 90% of VID specimens, indicating larger patches may be needed for more severe damage.

15. SUBJECT TERMS

composite materials, patch repair, sandwich structure, launch vehicle, damage tolerance, compression strength

16. SECURITY CLASSIFICATION OF:			17. LIMITATION OF ABSTRACT	18. NUMBER OF PAGES	19a. NAME OF RESPONSIBLE PERSON
a. REPORT	b. ABSTRACT	c. THIS PAGE			STI Help Desk at email: help@sti.nasa.gov
U	U	U	UU	38	19b. TELEPHONE NUMBER *(Include area code)* STI Help Desk at: 757–864–9658

National Aeronautics and
Space Administration
IS02
George C. Marshall Space Flight Center
Huntsville, Alabama 35812